ACS APPLIED MATERIALS & INTERFACES

Research Article

www.acsami.org

Thymine Functionalized Graphene Oxide for Fluorescence "Turn-off-on" Sensing of Hg^{2+} and I^- in Aqueous Medium

Diptiman Dinda, Bikash Kumar Shaw, and Shyamal Kumar Saha*

Department of Materials Science, Indian Association for the Cultivation of Science, Jadavpur, Kolkata 700032, India

Supporting Information

ABSTRACT: Selective detection of either mercury (Hg^{2+}) or iodide (I^-) ion using fluorescence turn-on or turn-off processes is an important area of research. In spite of intensive research, simultaneous detection of both mercury and iodide using fluorescence turn-off-on processes, high sensitivity and theoretical support concerning the mechanisms are still lacking. In the present work, graphene oxide is functionalized by thymine to realize simultaneous detection of both Hg^{2+} and I^- selectively using fluorescence turn-off-on mechanism. Ultra high sensitivity to the extent of ppb level exploiting large surface area of graphene is achieved. DFT calculations also assist to realize the detailed mechanisms involving this PL quenching and also its regain during sensing of these ions in aqueous solution.

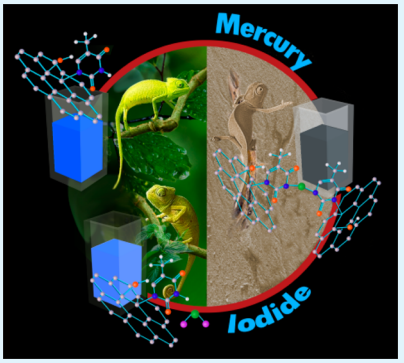

KEYWORDS: *functionalization, graphene oxide, fluorescence turn-off-on sensing, selectivity, DFT calculations*

INTRODUCTION

Heavy metal ion pollution has become a major concern to human health and ecology during the past decade.[1] Among different toxic metals, mercury (Hg^{2+}) is one of the most toxic pollutants in the earth.[2] According to United States Environment Protection Agency, every year ~60 000 tons of mercury is generated from natural and human sources, resulting in its incorporation into our food chain system.[3,4] It can easily pass through our skin and respiratory and gastrointestinal tissues and damage our central nervous system, causing brain damage, kidney failure, and various cognitive and motion disorders.[5,6] Similarly, iodide anion (I^-) has also drawn important attention in biological fields due to its essential role in micro nutrition and neurological and thyroid gland function for normal human growth. According to the World Health Organization, iodide deficiency also causes serious health disorders in the human body. Therefore, these adverse effects garner interests in designing new chemical routes for sensitive detection of Hg^{2+} and I^- ions.[7,8] The methods generally used to detect these ions include atomic absorption spectrometry, plasma-mass spectrometry, colorimetric strategies, capillary electrophoresis, and dithio-amide-functionalized lipid bilayers.[9−13] Most of these processes have limitations due to the interference from other metal ions, delayed response and a lack of usability in aqueous medium. Therefore, selective and sensitive detection of Hg^{2+} and I^- ions in water medium is really a challenging task.

Recently, fluorescence has become a powerful technique for detecting low concentrations of analytes due to its high accuracy, sensitivity, and simplicity.[14−19] Graphene, a monolayer of sp^2 carbons, has been extensively investigated due to its large surface area, superior electronic, mechanical properties, and exceptional thermal stability.[20,21] Graphene oxide (GO), an oxidized form of graphene with several functional groups like epoxy, hydroxyl, and carboxylic, is a more effective material where sensing applications are concerned.[22−24] Higher reactivity and solubility in suitable solvents make this material very special in different applications.[25−29] In spite of that, fluorescence-based sensing applications using GO are still in their infancy due to poor optical property.[30] During the past few years, several strategies have been developed to improve optical property using functionalization technique.[31−33] Therefore, it is quite interesting to use functionalized GO for the selective detection of Hg^{2+} and I^- ions at the low concentration limits.

Recently, some fluorescent nanomaterials have been used to detect mercury and iodide ions.[34−40] In spite of those, cost-effective production, stability, sensitivity, selectivity, and regeneration of the material particularly in aqueous medium are still to be improved. Mostly, the design of fluorescence turn-off-on systems for mercury and iodide probes is not an easy task as iodide has an intrinsic fluorescence quenching nature due to the heavy atom effect and lower binding affinity.[41,42] In addition, structural stability of the complex for this fluorescence turn-off-on mechanism has not yet been investigated using theoretical calculations in spite of few experimental results.

In this study, we have functionalized weak emissive GO at the epoxy sites by nucleic acid base thymine through normal S_N2 mechanism ensuing a new luminescent thymine functionalized reduced GO (T−rGO) material. We have successfully demonstrated the fluorescence turn-off-on sensing of Hg^{2+} and

Received: March 25, 2015
Accepted: June 22, 2015
Published: June 22, 2015

DOI: 10.1021/acsami.5b02603
ACS Appl. Mater. Interfaces 2015, 7, 14743−14749

I^- ions in aqueous medium as shown in Scheme 1. Here, the complete quenching of fluorescence intensity occurs selectively

Scheme 1. Fluorescence Turn-off-on Sensing of Hg^{2+} and I^- by T−rGO

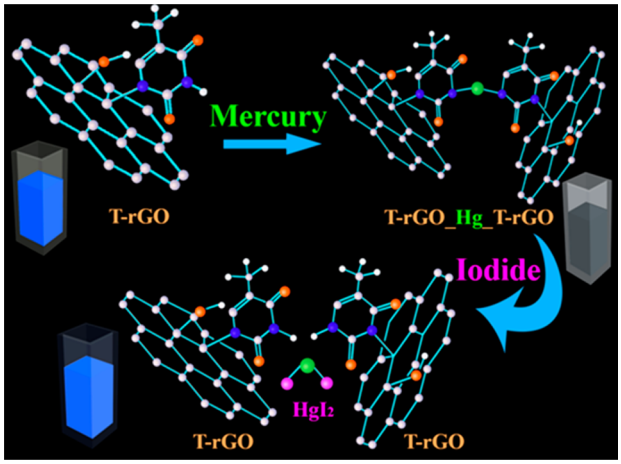

after addition of 40 μM Hg^{2+} solution and also regained by addition of 80 μM iodide salts in aqueous medium. The as-synthesized material is also very sensitive toward both mercury and iodide ions down to their nano molar concentrations. The density functional theory (DFT) calculations also help us to understand the structural stability and the nature of interactions between fluorophore T−rGO, Hg^{2+} and I^- ions during this turn-off-on selective fluorescence sensing.

RESULTS AND DISCUSSION

Photoluminescence Study. Following successful applications of the T−Hg^{2+}−T pairing, we have prepared a thymine-based novel graphene fluorophore nano probe. First, we have synthesized GO by modified Hummer's method and then, functionalized with thymine moieties using a simple S_N2 reaction mechanism. This results a bright blue emissive fluorophore (T−rGO) which gives an intense spectra at 448 nm when excited at 340 nm wavelength as shown in Figure 1a. During functionalization with thymine, the epoxy groups which contain nonradiative electron−hole (e−h) pairs are broken by amine group of thymine exhibiting such large enhancement in PL spectra. The compared PL spectra of GO and T−rGO is given in Figure S4 (Supporting Information). The as-synthesized material shows a strong PLE spectrum at 342 nm, shown in the inset of Figure 1a. From Figure 1b, we can also see a red shift in its peak position with change in excitation wavelength for this fluorophore. This observation also indicates surface passivation of GO during its functionalization.[33] The calculated QY of our synthesized T−rGO is ~22.47%. All the calculations are given in the Supporting Information.

Selective Mercury Sensing by Fluorescence Quenching. Prior to evaluating the metal ion selectivity, we have used this material for the detection of Hg^{2+} ions in aqueous solution. We have used mercury metal ions as a fluorescence (PL) quencher during this sensing experiment. We have added aqueous solutions of Hg^{2+} ions to the aqueous dispersion of T−rGO at pH7 (buffer solution of potassium dihydrogen phosphate/disodium hydrogen phosphate dihydrate). An immediate fluorescence quenching (~14%) is observed after incubation of only 2 μM Hg^{2+} solutions owing to strong

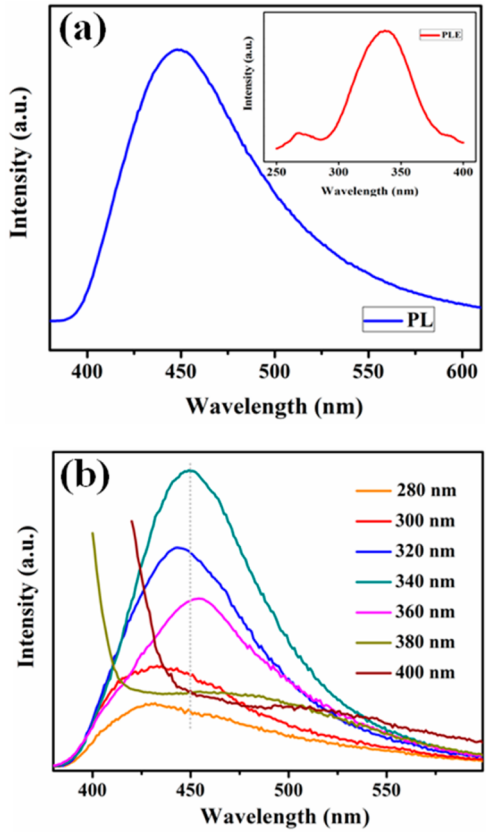

Figure 1. (a) Fluorescence spectra of T−rGO, (inset) its PLE spectrum, and (b) excitation dependent PL spectra.

binding interaction between thymine moiety and Hg^{2+} ions. From Figure 2a, it is seen that the fluorescence is quenched totally after addition of 40 μM Hg^{2+} solutions. To check the selectivity of T−rGO toward Hg^{2+}, we have also carried out PL quenching experiment with different metal ions such as Fe^{3+}, Ni^{2+}, Cu^{2+}, Fe^{2+}, Co^{2+}, Mn^{2+}, Pb^{2+}, Al^{3+}, Na^+, K^+, Ag^+, and so on. All the other ions show very moderate PL quenching compared to Hg^{2+} after 40 μM, as shown in Figure 2b. These results indicate the strong selectivity of T−rGO toward Hg^{2+}.

We have also studied the quenching experiment for Hg^{2+} in the presence of other metal ions. We initally added 20 μM aqueous solutions of different metal ions to the aqueous dispersion of T−rGO to access more vacant binding sites, followed by the addition of 20 μM Hg^{2+} solution. The experimental results in Figure 3a show that all the metal ions, including mercury, show quite similar quenching effect along with bare 20 μM of Hg^{2+}. These results are worth noting with the fact that the T−rGO fluorescent probe is expediently combined with mercury(II) ion via T−Hg^{2+}−T interaction causing such sensitive PL quenching compared to other metal ions.[43]

The fluorescence quenching efficiency is also analyzed by Stern−Volmer plot using equation $I_0/I = K_{SV}[Q] + 1$, where I_0 and I are fluorescence intensities before and after addition of different analytes, [Q] is the molar concentration of analytes added and K_{SV} is the quenching constant (M^{-1}). From Figure 3(b), it is seen that Hg^{2+} shows an exponential S−V curve whereas others show typical linear curve. At lower concentration, the S−V plot of Hg^{2+} is close to linear, but with increase in concentration it completely deviates from linearity and increases almost exponentially. Whereas, all the plots for

DOI: 10.1021/acsami.5b02603
ACS Appl. Mater. Interfaces 2015, 7, 14743−14749

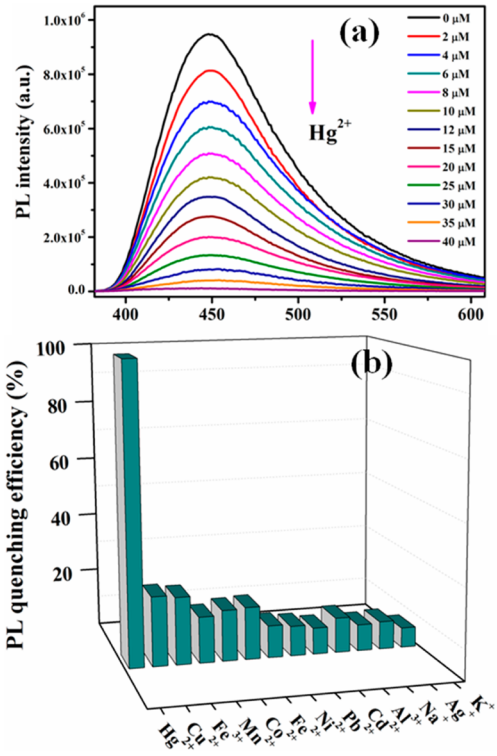

Figure 2. (a) Fluorescence quenching experiment after the addition of different micromolar Hg^{2+} solution to 5 mL T−rGO solution at pH 7 and (b) quenching efficiency with different metal ions.

other metal ions remain linear at higher concentrations. This statistics resolutely props up the selectivity of T−rGO with Hg^{2+}. Once the selectivity of the T−rGO fluorophore for Hg^{2+} is established, it is of interest to determine the limit of quantification for the detection of mercury(II). This system has a limit of quantification down to 400 ppb that implies the super sensitivity of this fluorophore over other reported materials. The experimental data and calculations are given in Figure S5a (Supporting Information).

Changes during Hg^{2+} Sensing. After the attachment of thymine molecules, T−rGO has become a fluorescent active material. Now, this fluorophore acts as an electron donor center during photoinduced electron transfer (PET) mechanism. As the Hg^{2+} ions have very natural tendency to bind with the nitrogen atoms of thymine molecules, they stabilize forming T−Hg^{2+}−T-like base pairs. Now, during PL experiments, electrons are easily transferred from the electron-rich fluorophore (T−rGO) to electron-deficient Hg^{2+} ions following PET mechanism. This causes a large quench in fluorescence of the fluorophore T−rGO material. To clarify this fact we also performed, time-correlated single-photon counting (TCSPC) study, as decay time measurements are highly sensitive during PL quenching experiments. The calculated average decay time for T−rGO fluorophore is 10.4 ns, shown in Table S1 (Supporting Information). After the addition of Hg^{2+}, the decay time of the fluorophore decreases gradually. Finally, it reduces to 7.97 ns after addition of 40 μM Hg^{2+}, shown in Figure 4a,b. This result stoutly resembles the strong binding ability of Hg^{2+} to the thymine gr. of T−rGO composite ensuing tremendous PL quenching.

From the UV−vis spectrum in Figure S6 (Supporting Information), it is also seen that the peak at 260 nm of T−rGO is gradually decreased after addition of Hg^{2+} solution owing to

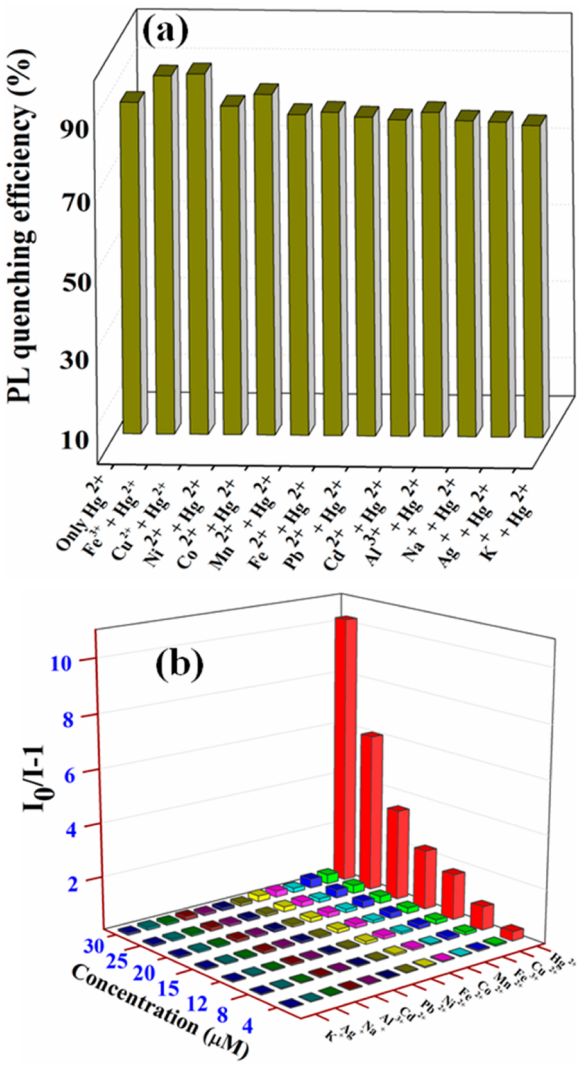

Figure 3. (a) PL quenching efficiency of T−rGO in the presence of 20 μM of different metal ions followed by 20 μM of Hg^{2+} ion and (b) Stern−Volmer plot for those metal ions.

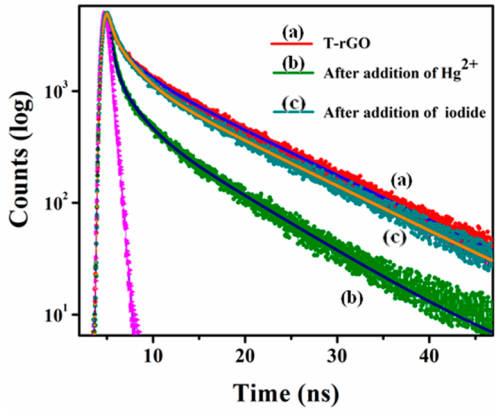

Figure 4. Decay time of (a) T−rGO, (b) T−rGO after the addition of Hg^{2+} solution, and (c) T−rGO/Hg^{2+} system after the addition of iodide solution during TCSPC measurements.

the interaction between Hg^{2+} and amine group of thymine base. The FTIR spectra of T−rGO in Figure S7 (Supporting Information), also support the formation of coordinative interaction after addition of Hg^{2+}. The shifting of C−N

DOI: 10.1021/acsami.5b02603
ACS Appl. Mater. Interfaces 2015, 7, 14743−14749

stretching vibration from 1230 to 1213 cm^{-1} resembles strong binding interaction between mercury ion and nitrogen atom of thymine base. During this PL quenching experiment, electrons are transferred from graphene-based fluorophore to mercury ions causing shifting of D and G bands. As a result, the G band is blue-shifted from 1584 to 1593 cm^{-1}, and D band is red-shifted from 1366 to 1355 cm^{-1}, as shown in Figure S8 (Supporting Information).

Selective Iodide Sensing by Restoring Quenched PL. We further examine that T−rGO_Hg system can also be used as a PL-responsive probe for iodide sensing as the quenched fluorescence of the complex is restored in the presence of iodide salt. We have measured the recovered fluorescence spectra of T−rGO_Hg system in the presence of double volume of iodide solution as one Hg^{2+} ion binds with two iodide ions forming HgI_2 salt. With the addition of iodide solution, the fluorescence emission of the complex increases gradually. The binding constant for thymine and Hg^{2+} is $\sim 10^6$, while for Hg^{2+} and I^- it is $>10^{29}$.[44] Therefore, this high binding affinity guides the formation of HgI_2 molecule making T−rGO nanoprobe free. This helps to stop PET from electron rich fluorophore to electron deficient moiety resulting such enhancement in the PL property during fluorescent "turn-on" sensing. We have been able to regain its fluorescence efficiency up to 96% after addition of 80 μM iodide salt, as shown in Figure 5a. To elucidate the selectivity of the T−rGO_Hg system toward iodide salt, we have carried out turn-on fluorescent experiments with different anions like F^-, Cl^-, Br^-, SO_4^{2-}, NO_3^-, CO_3^{2-}, CH_3COO^-, and PO_4^{3-}. From Figure 5b, it is seen that the fluorescence enhancement for other anions are quite low compared to iodide. These results strongly reveal that T−rGO_Hg system is also very selective toward the sensing of iodide salt.

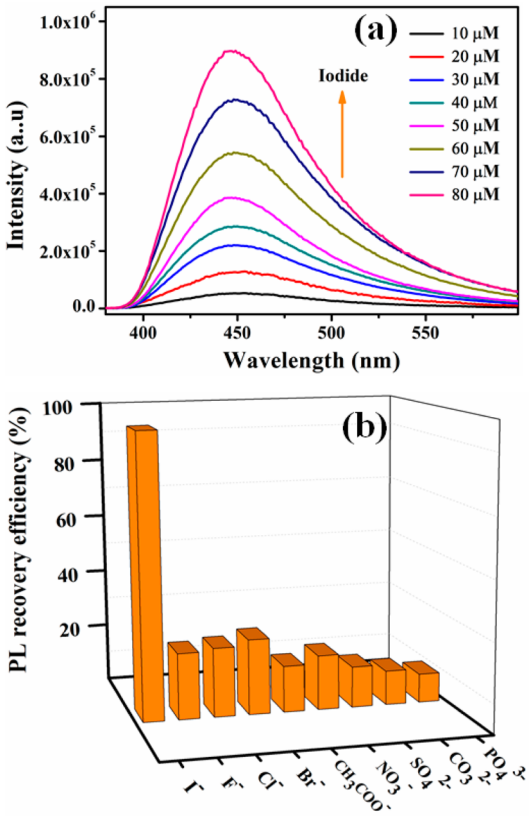

Figure 5. (a) Recovery of PL by different micro molar iodide solutions after quenched by 40 μM of Hg^{2+} solution at pH 7 and (b) PL recovery efficiency with different anions.

To investigate the interference of other anions during this PL recovery experiment, we measured the PL recovery efficiency of T−rGO/Hg^{2+} with iodide ions in the presence of different anions. We have done all these experiments with initial 40 μM of different anions followed by another 40 μM of iodide solutions. From Figure S9 (Supporting Information), it is seen that bare iodide ion has very promising recovery efficiency in the presence of other anions. So, all the other anions have very little interference toward the T−rGO/Hg^{2+} system during PL recovery experiments by iodide ion.

To consolidate this, we conducted TCSPC measurements after the addition of iodide salt. The value of lifetime gradually increases from 7.9 to 10.2 ns after the addition of 80 μM of iodide solution, shown in Figure 4c. These results indicate that Hg(II) form strong complex with iodine (HgI_2) making amine group of thymine free during this "turn-on" sensing. According to the WHO, for a healthy human being, the maximum recommended iodide concentrations in drinking water and in the human urinary system are 18 and 100−200 $\mu g\ L^{-1}$, respectively.[45] For practical application, we have also measured the detection limit of iodide for our material. From Figure S5b (Supporting Information), we see that the detection limit of iodide is 1.27 ppm, which is well below the allowed concentration level in drinking water.

To verify the selectivity and sensitivity of T−rGO in real samples, we carried out sensing experiments with local tap water of Jadavpur area by adding different amounts of mercury and iodide ions to it. We measured their PL recovery efficiency, which is shown in Table S2 (Supporting Information). Greater than 90% recovery efficiency in tap water is well in agreement with the selectivity of the sensor without any significant interference of other ions present in tap water.

DFT Study. Hg^{2+} can form stable structure with thymine moiety of T−rGO system via T−Hg^{2+}−T interaction compared to other metal ions resulting strong PL quenching. When iodide ions are added to that solution, iodide can strongly bind to those captured Hg^{2+} ions, making thymine groups free, and the quenched PL is recovered as shown in Scheme 1. To confirm this, we theoretically investigated the total experiment by DFT technique using the B3LYP/6-31G method in the GAUSSIAN 03 software package. For this, we first optimized T−rGO system (Figure S10, Supporting Information) and then incorporate different metal ions in it. The DFT optimized structure in Figure 6a strongly supports that Hg^{2+} can form very stable structure with T−rGO via T−Hg^{2+}−T interaction. We have also carried out this optimization experiment with other metal ions such as Fe^{3+}, Ni^{2+}, Co^{2+}, Mn^{2+}, Ag^+, and Na^+. The optimized structures for all metal ions are shown in Figures S11−S16 (Supporting Information). To obtain the most stable structure, we also calculate the highest occupied molecular orbital (HOMO) energy levels for all the systems. The stabilized HOMO energy levels for all the systems are summarized in Table 1. From Table 1, the most stable HOMO energy level is found for the T−rGO_Hg_T−rGO system as T−rGO moiety forms most stable complex with Hg(II) ion compared to other metal ions. Now, when we incorporate iodide ions to the optimized T−rGO_Hg_T−rGO system, I^- strongly coordinates with that captured Hg^{2+} ion, forming stable HgI_2 molecule, as shown in Figure 6b. As a result, the engaged thymine moieties in the T−Hg−T system

DOI: 10.1021/acsami.5b02603
ACS Appl. Mater. Interfaces 2015, 7, 14743−14749

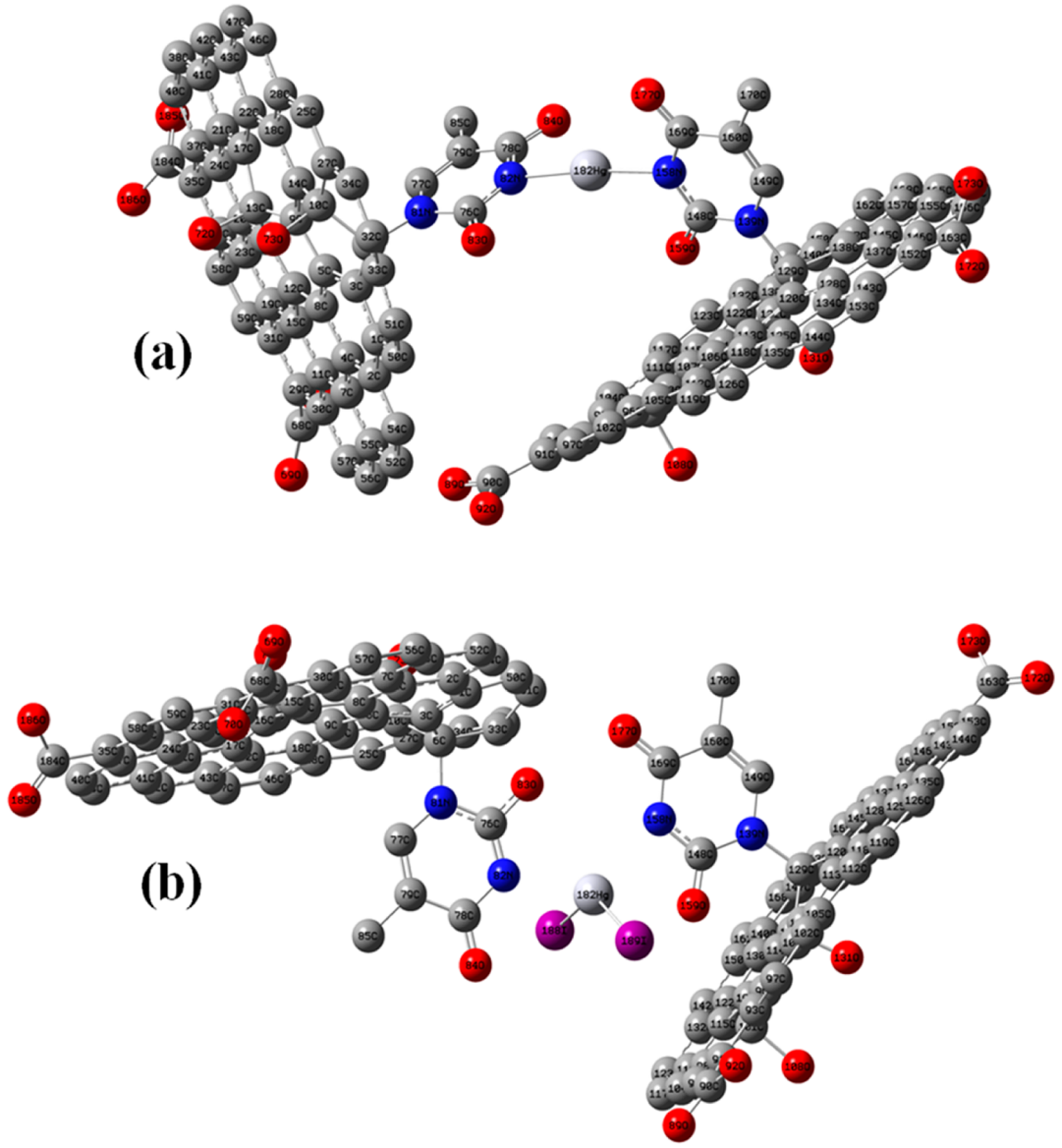

Figure 6. DFT optimized structure of T−rGO after addition of (a) Hg^{2+} and (b) I^- ions.

Table 1. HOMO Energy Levels of Optimized T−rGO System with Different Metal Ions

optimized structures	band energy (eV) HOMO	LUMO
only T−rGO	−4.81	−4.01
with Hg^{2+}	−4.55	−3.88
Ni^{2+}	−4.28	−3.98
Mn^{2+}	−4.32	−3.56
Co^{2+}	−4.38	−3.41
Fe^{3+}	−4.31	−3.91
Ag^{+}	−4.39	−3.98
Na^{+}	−4.32	−3.71
T−rGO/Hg^{2+} system after addition of I^- solution	−4.96	−4.04

become free to reorganize T−rGO moiety. So, the DFT calculations strongly support our proposed mechanism for T−rGO system and its selectivity toward Hg^{2+} and I^- ions during this fluorescence "turn-off-on" sensing in aqueous medium.

CONCLUSION

In summary, we have synthesized a new fluorescent probe through the functionalization of graphene oxide and successfully designed a new fluorescent "turn-off-on" based platform for the detection of mercury(II) and iodide(I) ions in aqueous medium. Owing to the strong binding interaction of T−Hg^{2+}−T base pair, mercury selectively quenches the fluorescence of our graphene-based fluorophore (T−rGO). The presence of other metal ions does not hinder the detection of Hg^{2+}. Furthermore, the addition of iodide salt recovers the quenched fluorescence making very stable HgI_2 complex with Hg^{2+}. Our developed system is able to detect Hg^{2+} and I^- at nano molar concentration level. We have also proved our proposed mechanism of fluorescence sensing by DFT calculations. Finally, very simple, economic, higher selectivity, and sensitive detection ability make this graphene based fluorophore a suitable material for the selective detection of mercury and iodide ions in aqueous medium.

DOI: 10.1021/acsami.5b02603
ACS Appl. Mater. Interfaces 2015, 7, 14743−14749

EXPERIMENTAL SECTION

Details including the synthesis process, required chemicals, fluorescence experimental details, characterizations, and microstructural analysis of the prepared T−rGO material are given in Supporting Information.

ASSOCIATED CONTENT

Supporting Information

Details of experimental section including synthesis procedure, required chemicals, fluorescence experimental details, characterizations and microstructural analysis of our prepared T−rGO material; detection limit data for mercury and iodide; microstructural change after addition of mercury; TCSPC calculations and DFT optimized structures. The Supporting Information is available free of charge on the ACS Publications website at DOI: 10.1021/acsami.5b02603.

AUTHOR INFORMATION

Corresponding Author

*E-mail: cnssks@iacs.res.in.

Notes

The authors declare no competing financial interest.

ACKNOWLEDGMENTS

D.D. and B.K.S. acknowledge CSIR-SPM and CSIR, respectively, for awarding their fellowships. S.K.S. acknowledges DST, project no. SR/S2/CMP-0097/2012.

REFERENCES

(1) Renzoni, A.; Zino, F.; Franchi, E. Mercury Levels along the Food Chain and Risk for Exposed Populations. *Environ. Res.* **1998**, *77*, 68−72.

(2) Descalzo, A. B.; Martinez-Màñez, R.; Radeglia, R.; Rurack, K.; Soto, J. Coupling Selectivity with Sensitivity in an Integrated Chemosensor Framework: Design of a Hg^{2+}-Responsive Probe, Operating above 500 nm. *J. Am. Chem. Soc.* **2003**, *125*, 3418−3419.

(3) Pacyna, E. G.; Pacyna, J. M.; Pirrone, N. European Emissions of Atmospheric Mercury from Anthropogenic Sources in 1995. *Atmos. Environ.* **2001**, *35*, 2987−2996.

(4) Liu, J.; Lu, Y. Rational Design of "Turn-On" Allosteric DNAzyme Catalytic Beacons for Aqueous Mercury Ions with Ultrahigh Sensitivity and Selectivity. *Angew. Chem.* **2007**, *119*, 7731−7734.

(5) Grandjean, P.; Weihe, P.; White, R. F.; Debes, F. Cognitive Performance of Children Prenatally Exposed to "Safe" Levels of Methylmercury. *Environ. Res.* **1998**, *77*, 165−172.

(6) Takeuchi, T.; Morikawa, N.; Matsumoto, H.; Shiraishi, Y. A Pathological Study of Minamata disease in Japan. *Acta Neuropathol.* **1962**, *2*, 40−57.

(7) Ho, H. A.; Leclerc, M. New Colorimetric and Fluorometric Chemosensor Based on a Cationic Polythiophene Derivative for Iodide-Specific Detection. *J. Am. Chem. Soc.* **2003**, *125*, 4412−4413.

(8) Taurog, A. M. *The Thyroid: A Fundamental and Clinical Text*; Lippincott, Williams & Wilkins, Philadelphia, 2000, 61−85.

(9) Chen, L.; Li, J.; Chen, L. Colorimetric Detection of Mercury Species Based on Functionalized Gold Nanoparticles. *ACS Appl. Mater. Interfaces* **2014**, *6*, 15897−15904.

(10) Li, Y. J.; Tseng, Y. T.; Unnikrishnan, B.; Huang, C. C. Gold-Nanoparticles-Modified Cellulose Membrane Coupled with Laser Desorption/Ionization Mass Spectrometry for Detection of Iodide in Urine. *ACS Appl. Mater. Interfaces* **2013**, *5*, 9161−9166.

(11) Liu, H. W.; Jiang, S. J.; Liu, S. H. Determination of Cadmium, Mercury and Lead in Seawater by Electrothermal Vaporization Isotope Dilution Inductively Coupled Plasma Mass Spectrometry. *Spectrochim. Acta, Part B* **1999**, *54*, 1367−1375.

(12) Sasaki, D. Y.; Padilla, B. E. Dithioamide Metal Ion Receptors on Fluorescent Lipid Bilayers for the Selective Optical Detection of Mercuric Ion. *Chem. Commun.* **1998**, *15*, 1581−1582.

(13) Du, Y.; Liu, R.; Liu, B.; Wang, S.; Han, M. Y.; Zhang, Z. Surface-Enhanced Raman Scattering Chip for Femtomolar Detection of Mercuric Ion (II) by Ligand Exchange. *Anal. Chem.* **2013**, *85*, 3160−3165.

(14) Guo, X.; Qian, X.; Jia, L. A Highly Selective and Sensitive Fluorescent Chemosensor for Hg^{2+} in Neutral Buffer Aqueous Solution. *J. Am. Chem. Soc.* **2004**, *126*, 2272−2273.

(15) Li, H.; Zhaia, J.; Sun, X. Nano-C60 as a Novel, Effective Fluorescent Sensing Platform for Mercury(II) Ion Detection at Critical Sensitivity and Selectivity. *Nanoscale* **2011**, *3*, 2155−2157.

(16) Nolan, E. M.; Lippard, S. J. A "Turn-On" Fluorescent Sensor for the Selective Detection of Mercuric Ion in Aqueous Media. *J. Am. Chem. Soc.* **2003**, *125*, 14270−14271.

(17) Maiti, S.; Pezzato, C.; Martin, S. G.; Prins, L. J. Multivalent Interactions Regulate Signal Transduction in a Self-Assembled Hg^{2+} Sensor. *J. Am. Chem. Soc.* **2014**, *136*, 11288−11291.

(18) Yuan, X.; Yeow, T. J.; Zhang, Q.; Lee, J. Y.; Xie, J. Highly Luminescent Ag^{+} Nanoclusters for Hg^{2+} Ion Detection. *Nanoscale* **2012**, *4*, 1968−1971.

(19) Zhang, K.; Zhou, H.; Mei, Q.; Wang, S.; Guan, G.; Liu, R.; Zhang, J.; Zhang, Zhongping Instant Visual Detection of Trinitrotoluene Particulates on Various Surfaces by Ratiometric Fluorescence of Dual-Emission Quantum Dots Hybrid. *J. Am. Chem. Soc.* **2011**, *133*, 8424−8427.

(20) Yoo, E.; Kim, J.; Hosono, E.; Zhou, H.; Kudo, T.; Honma, I. Large Reversible Li Storage of Graphene Nanosheet Families for Use in Rechargeable Lithium Ion Batteries. *Nano Lett.* **2008**, *8*, 2277−2282.

(21) Kim, K. S.; Zhao, Y.; Jang, H.; Lee, S. Y.; Kim, J. M.; Kim, K. S.; Ahn, J. H.; Kim, P.; Choi, J. Y.; Hong, B. H. Large-Scale Pattern Growth of Graphene Films for Stretchable Transparent Electrodes. *Nature* **2009**, *457*, 706−710.

(22) Mkhoyan, K. A.; Contryman, A. W.; Silcox, J.; Stewart, D. A.; Eda, G.; Mattevi, C.; Miller, S.; Chhowalla, M. Atomic and Electronic Structure of Graphene-Oxide. *Nano Lett.* **2009**, *9*, 1058−1063.

(23) Gupta, B. K.; Thanikaivelan, P.; Narayanan, T. N.; Song, L.; Gao, W.; Hayashi, T.; Reddy, A. L. M.; Saha, A.; Shanker, V.; Endo, M.; Martí, A. A.; Ajayan, P. M. Optical Bifunctionality of Europium-Complexed Luminescent Graphene Nanosheets. *Nano Lett.* **2011**, *11*, 5227−5233.

(24) Mei, Q.; Zhang, Z. Photoluminescent Graphene Oxide Ink to Print Sensors onto Microporous Membranes for Versatile Visualization Bioassays. *Angew. Chem., Int. Ed.* **2012**, *51*, 5602−5606.

(25) Zhu, Y.; Murali, S.; Cai, W.; Li, X.; Suk, J. W.; Potts, J. R.; Ruof, R. S. Graphene and Graphene Oxide: Synthesis, Properties, and Applications. *Adv. Mater.* **2010**, *22*, 3906−3924.

(26) Chen, D.; Feng, H.; Li, J. Graphene Oxide: Preparation, Functionalization, and Electrochemical Applications. *Chem. Rev.* **2012**, *112*, 6027−6053.

(27) Dinda, D.; Saha, S. K. Sulfuric Acid Doped Poly Diaminopyridine/Graphene Composite to Remove High Concentration of Toxic Cr(VI). *J. Hazard. Mater.* **2015**, *291*, 93−101.

(28) Loh, K. P.; Bao, Q. L.; Eda, G.; Chhowalla, M. Graphene Oxide as a Chemically Tunable Platform for Optical Applications. *Nat. Chem.* **2010**, *2*, 1015−1024.

(29) Bhattacharya, S.; Dinda, D.; Saha, S. K. Role of Trap States on Storage Capacity in a Graphene/MoO_3 2D Electrode Material. *J. Phys. D: Appl. Phys.* **2015**, *48*, 145303.

(30) Banerjee, M.; Gupta, A.; Saha, S. K.; Chakravorty, D. 1-Aza-15-Crown-5 Functionalized Graphene Oxide for 2D Graphene-Based Li +-ion Conductor. *Small* **2015**, DOI: 10.1002/smll.201500200.

(31) Dinda, D.; Gupta, A.; Shaw, B. K.; Sadhu, S.; Saha, S. K. Highly Selective Detection of Trinitrophenol by Luminescent Functionalized Reduced Graphene Oxide through FRET Mechanism. *ACS Appl. Mater. Interfaces* **2014**, *6*, 10722−10728.

(32) Singh, S. K.; Singh, M. K.; Kulkarni, P. P.; Sonkar, V. K.; Grácio, J.; Dash, D. Amine-Modified Graphene: Thrombo-Protective Safer Alternative to Graphene Oxide for Biomedical Applications. *ACS Nano* **2012**, *6*, 2731−2740.
(33) Mei, Q.; Zhang, K.; Guan, G.; Liu, B.; Wang, S.; Zhang, Z. Highly Efficient Photoluminescent Graphene Oxide with Tunable Surface Properties. *Chem. Commun.* **2010**, *46*, 7319−7321.
(34) Du, F.; Zeng, F.; Ming, Y.; Wu, S. Carbon Dots-Based Fluorescent Probes for Sensitive and Selective Detection of Iodide. *Microchim. Acta* **2013**, *180*, 453−460.
(35) Ma, B.; Zeng, F.; Zheng, F.; Wu, S. A Fluorescence Turn-on Sensor for Iodide Based on a Thymine−Hg^{II}−Thymine Complex. *Chem. - Eur. J.* **2011**, *17*, 14844−14850.
(36) Chen, S.; Wang, P.; Jia, C.; Lin, Q.; Yuan, W. A Mechanosynthesized, Sequential, Cyclic Fluorescent Probe for Mercury and Iodide Ions in Aqueous Solutions. *Spectrochim. Acta, Part A* **2014**, *133*, 223−228.
(37) Mitra, A.; Mittal, A. K.; Rao, C. P. Carbohydrate Assisted Fluorescence Turn-On Gluco−Imino−Anthracenyl Conjugate as a Hg(II) Sensor in Milk and Blood Serum Milieu. *Chem. Commun.* **2011**, *47*, 2565−2567.
(38) Bandela, A.; Chinta, J. P.; Rao, C. P. Role of the Conformational Changes Brought in the Arms of the 1, 3-di-Capped Conjugate of Calix[4]arene (L) in Turning on the Fluorescence of L by Hg^{2+}. *Dalton Trans.* **2011**, *40*, 11367−11370.
(39) Li, Z.; Yu, H.; Bian, T.; Zhao, Y.; Zhou, C.; Shang, L.; Liu, Y.; Wu, L. Z.; Tung, C. H.; Zhang, T. Highly Luminescent Nitrogen-Doped Carbon Quantum Dots as Effective Fluorescent Probes for Mercuric and Iodide Ions. *J. Mater. Chem. C* **2015**, *3*, 1922−1928.
(40) Kong, F.; Meng, X.; Chu, R.; Xu, K.; Tang, B. A Turn-On Fluorescence Probe for Imaging Iodide in Living Cells Based on an Elimination Reaction. *Chem. Commun.* **2015**, *51*, 6925−6927.
(41) Wang, L.; Fang, G.; Ye, D.; Cao, D. Carbazole and Triazole-Containing Conjugated Polymer as a Visual and Fluorometric Probe for Iodide and Mercury. *Sens. Actuators, B* **2014**, *195*, 572−580.
(42) Martínez-Máñez, R.; SancenÓn, F. Fluorogenic and Chromogenic Chemosensors and Reagents for Anions. *Chem. Rev.* **2003**, *103*, 4419−4476.
(43) Tanaka, Y.; Oda, S.; Yamaguchi, H.; Kondo, Y.; Kojima, C.; Ono, A. ^{15}N−^{15}N J-Coupling across Hg^{II}: Direct Observation of Hg^{II}-Mediated T−T Base Pairs in a DNA Duplex. *J. Am. Chem. Soc.* **2007**, *129*, 244−245.
(44) Torigoe, H.; Ono, A.; Kozasa, T. Hg^{II} Ion Specifically Binds with T:T Mismatched Base Pair in Duplex DNA. *Chem.—Eur. J.* **2010**, *16*, 13218−13225.
(45) Hetzel, B. S. Eliminating Iodine Deficiency Disorders—The Role of the International Council in the Global Partnership. *Bull. W.H.O.* **2002**, *80* (5), 410−417.

DOI: 10.1021/acsami.5b02603
ACS Appl. Mater. Interfaces 2015, 7, 14743−14749